NON DESTRUCTIVE ANALYSIS OF CONCRETE FOR CORROSION STUDIES UTILIZING NUCLEAR TECHNIQUE

A. A. Naqvi[1], M. M. Nagadi[1], M. A. Garwan[1], O.S. B. Al-Amoudi[2], M. Maslehuddin[3], Khateeb-ur-Rehman[1] and M. Raashid[1]

[1] Department of Physics,

[2] Department of Civil Engineering,

[3] Center for Engineering Research, Research Institute

King Fahd University of Petroleum and Minerals,

Dhahran 31261, Saudi Arabia

ABSTRACT

Chloride-induced reinforcement corrosion is the principal cause of deterioration of concrete structures in the Arabian Gulf and the world over. Preventive measures against corrosion require maintaining the chloride and sulfur concentration in concrete below the threshold limits specified by the standards. This requires monitoring the chloride and sulfate concentration in concrete, and a non-destructive technique is preferable for this purpose. The Prompt Gamma Neutron Activation Analysis (PGNAA) technique can be used to monitor concentration of corrosive elements in concrete samples. An accelerator-based PGNAA setup has been developed to measure the chloride and sulfate concentration in concrete. The PGNAA technique has been used successfully to measure the elemental composition of concrete samples. In this regard several studies were under taken to determine calcium, silicon, chloride and sulfur in concrete specimens. Furthermore, the concentration of compounds, such as such as lime, silica, etc. was also determined. Results of these studies along with the facility description are presented in this talk.

1. INTRODUCTION

Deterioration of concrete structures due to reinforcement corrosion, which is mainly attributed to the diffusion of chloride ions to the steel surface, has been recognized as the number one durability problem facing the construction industry in the Arabian Gulf and many other parts of the world [1-5]. Pozzolanic materials, such as fly ash and silica fume, are added to concrete as partial replacement of Portland cement to make it dense and hence minimize reinforcement corrosion [6-9]. However, since reinforcement corrosion is caused due to the chloride ions it is necessary to monitor their concentration. However, the available techniques to quantify chloride ions in concrete, in particular the wet analysis methods [10], tend to be inaccurate due to the small sample size and the associated uncertainties during sampling and testing stages. Other techniques, such as PGNAA [11-19] and X-ray fluorescence (XRF) technique [11], can be utilized to determine the elemental composition of bulk samples. Both these techniques have their own advantages and limitations. The XRF technique, which requires specialized sampling methodology and sample preparation, has difficulties in analyzing low atomic number elements, such as C and O. Also this technique is excluded from the non-destructive category. On the other hand, the PGNAA technique is a fast and multi-elemental nuclear technique for analysis of bulk materials [11-24]. This technique is accurate enough to determine the concentration of light elements, such as C, S, F, Al, Si, P, Cl, Ca, Va and Fe in the range of 0.1% to 50% [11]. Another main advantage of this technique is its capability of analyzing very large samples. An accelerator-based PGNAA setup has been developed at King Fahd University of Petroleum and Minerals (KFUPM), Dhahran, Saudi Arabia, to analyze elemental composition of concrete specimens using a moderator [17-24]. In the following paragraph the facility development is presented along with a brief description of the research results achieved with this facility for the analysis of fly ash cement concrete specimens [24], analysis of chloride in Portland cement concrete [20], measurement of lime to silica ratio in concrete [21], and measurement of sulfur in concrete [22] has been explained.

2. KFUPM PGNAA SETUP

The elemental analysis of large samples of bulk materials at KFUPM accelerator-based PGNAA setup is carried out via prompt gamma rays excited through capture of thermal neutrons [17]. Thermal neutrons are produced at the sample through moderation from external moderator surrounding the cylindrical sample. The moderator is placed between a 2.8 MeV neutrons target (D(d,n) reaction target). The prompt gamma rays produced in the sample are detected by a cylindrical NaI gamma ray detector with dimensions of 25.5 cm x 25.5 cm (diameter x height) [26]. The cylindrical [17, 18, 20] as well as rectangular [21-24] moderators were tested in the PGNAA setup. Each of the moderators has a central cylindrical cavity, which can accommodate a cylindrical specimen. The design of the moderators was obtained from the Monte Carlo simulations carried out using the procedures described earlier [17]. In these calculations the yield of the prompt gamma rays from a Portland cement sample was optimized inside the detector volume as a function of sample radius, front moderator thickness and the sample length for the rectangular moderator [19]. The rectangular moderator, made of paraffin wax, has 49 cm x 49 cm (width x height) cross sectional area and 20 cm length. The moderator has a central cylindrical cavity, which can accommodate a 14 cm long cylindrical specimen with a maximum diameter of 25 cm. For a specimen with smaller diameter, a high density polyethylene plug is used, which fills the gap between the sample and the walls of the cavity [19]. Figure 1 shows the PGNAA setup with the rectangular moderator and the high density polyethylene plug with a sample with diameter less than the maximum diameter [23].

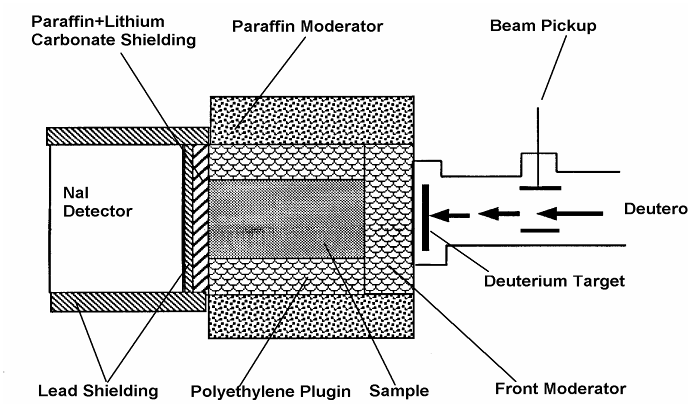

Figure 1: Schematic representation of the PGNAA setup used to measure prompt gamma ray yield.

In order to prevent undesired gamma rays and neutrons from reaching the detector, 3 mm thick lead shielding and 50 mm thick paraffin shielding are inserted between the moderator and the detector. The neutron shielding is made of a mixture of paraffin and lithium carbonate mixed in equal weight proportion [17]. Figure 2 shows the photograph of the KFUPM PGNAA setup.

Figure 2: Photograph of the PGNAA setup used to measure prompt gamma ray yield.

The gamma ray yield from the specimens is measured using a pulsed beam of 2.8 MeV neutrons, produced via the D(d,n) reaction. The deuteron pulse has a typical width of 5 ns and a repetition rate of 31.25 kHz and a beam current of 8 to 10 μA. The prompt γ-ray data are acquired in a PC based data acquisition system for a preset number of charges measured at the electrically-isolated neutron producing target. The detector signals are acquired in coincidence with a gate signal being derived from the beam pick-up signal [17-24].

3. Assessment of Fly Ash Concentration in Concrete specimens

The prompt gamma-ray yield from fly ash cement concrete specimens was measured to test the response of the PGNAA setup to measure the concentration of fly ash [24]. The size of the fly ash cement concrete specimen was calculated using Monte Carlo simulations [24]. Later, the results of Monte Carlo simulations were experimentally verified through gamma ray yield measurements as a function of specimen radius. Figures 3 show experimentally measured prompt γ-ray spectrum of five fly ash cement concrete specimens with different radii on an enlarged scale with energies higher than 3 MeV.

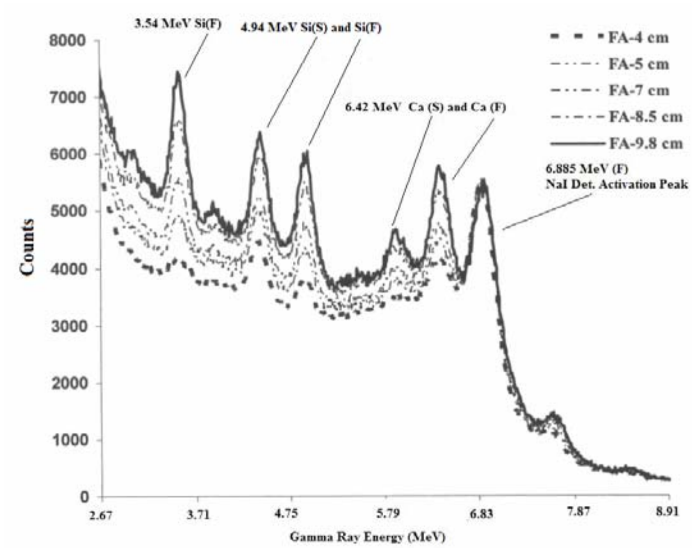

Figure 3. Experimentally measured prompt γ-rays spectrum of five fly ash cement concrete specimens with different radii.

Figure 3 shows the pulse height spectrum of prompt gamma-ray from fly ash cement concrete exhibiting silicon (3.54, 4.94 MeV) and calcium (6.42 MeV) peaks in the concrete specimen with energies higher than 3 MeV. The large peak at 6.885 MeV on the right end of the spectrum is the gamma-ray peaks from activation of sodium ^{23}Na and iodine ^{127}I in the NaI detector [32, 33]. Also shown in the Figure 3 are the full energy peaks of calcium Ca(F) at 6.42 MeV and two full energy prompt gamma ray peaks from silicon Si(F) at 4.94 MeV and 3.54 MeV respectively. The single escape peak of silicon Si(S) at 4.44 MeV energy is also shown in Figure 3. As shown in the Figure 3, with increasing radius of the specimen, the height of calcium and silicon peaks from the specimen also increases. This is clearly shown in Figure 3, where pulse height spectra of 6.42 MeV prompt gamma-ray from calcium and 3.54 and 4.94 MeV gamma-ray from silicon for fly ash cement concrete specimens with different radii are superimposed upon each other. The yield of the calcium gamma rays under the calcium peak in pulse height spectra of concrete specimen is plotted as a function of the sample radius in Figure 4.

The experimental yield in Figure 4 of the prompt gamma rays from the five specimens is shown by symbols while the calculated yield is shown by line.

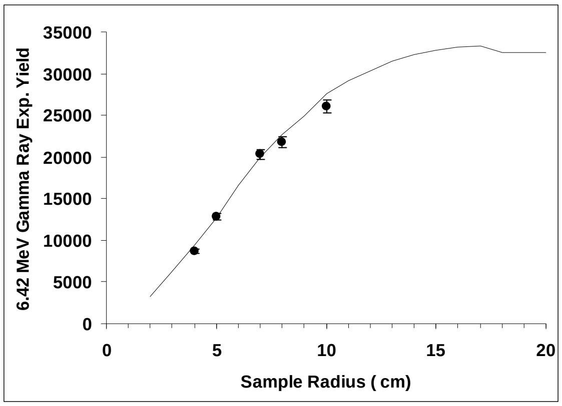

Figure 4: The experimental yield of the 6.42 MeV prompt gamma-ray for calcium in fly ash cement concrete specimen plotted as a function of specimen radius.

For the sake of fly ash concentration analysis in concrete, the prompt gamma ray yield from calcium and silicon was measured from five different fly ash cement concrete specimens containing fly ash concentration in 5, 10, 20, 40 and 80 wt % of Portland cement. Figure 5 shows pulse height spectra of fly ash cement concrete with 5 wt % (FA-005N shown with dashed line) and 80 wt. % (FA-080NN shown with solid line) superimposed on each other [24].

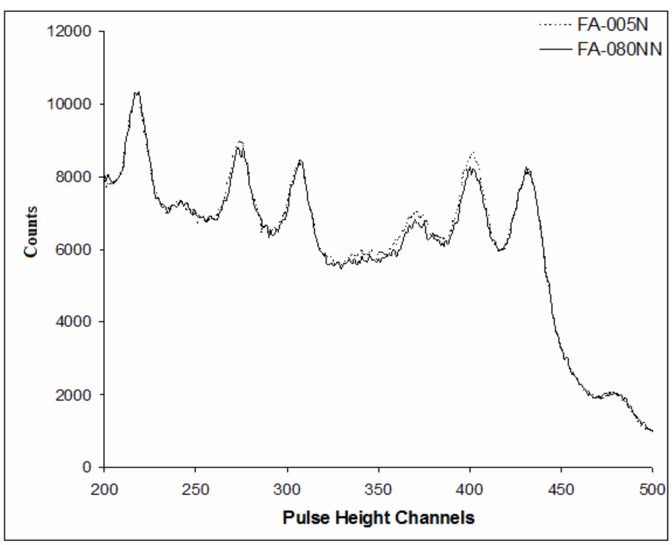

Figure 5: Prompt gamma-rays pulse height spectra for 5 wt. % and 80 wt. % fly ash fly ash cement concrete specimens with gamma energies above 3 MeV.

The peak height of calcium in fly ash cement concrete specimens decreases with increasing concentration of fly ash in the concrete. This is due to smaller concentration of calcium in fly ash as compared to Portland cement. The average calcium concentration of the fly ash and Portland cement mixture decreases with increasing fly ash concentration. Reverse is the case for concentration of silicon in concrete, which increases with increasing concentration of fly ash in the concrete. Figure 6 shows the normalized yield of 6.42 MeV prompt gamma ray for calcium in the five fly ash cement concrete specimens measured as a function of the fly ash concentration. The solid line shows normalized-calculated yield of the 6.42 MeV gamma-rays for five concrete specimens obtained through Monte Carlo calculations.

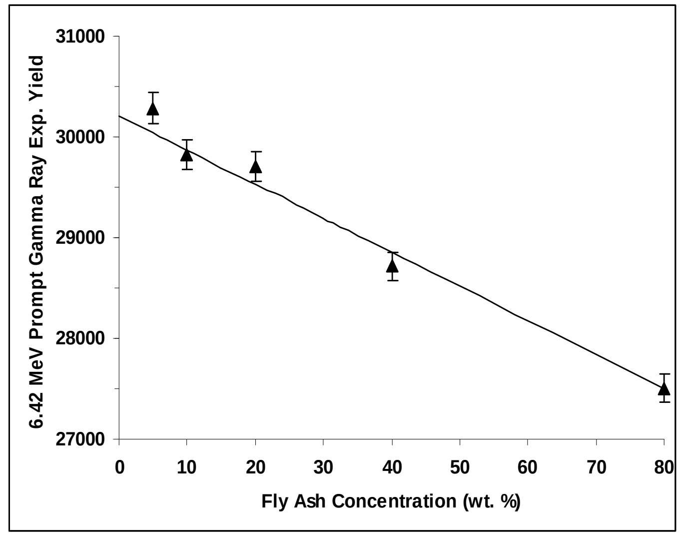

Figure 6: Experimental yield of 6.42 MeV gamma-rays from calcium in the five fly ash cement concrete specimens plotted as a function of fly ash concentration.

As expected, the gamma ray yield of calcium decreased with increasing concentration of fly ash in concrete. The solid lines in Figure 6 shows calculated yield of the 6.42 MeV prompt gamma ray from calcium obtained through Monte Carlo simulations.

4. Assessment of Chloride Contamination in the Portland cement concrete

The chloride concentration in a Portland cement concrete specimen was measured using the Small Sample Moderator (SSM) assembly [17, 18, 20] of the KFUPM PGNAA setup. The SSM PGNAA setup [20] consists of a 14 cm long cylindrical polyethylene container with a 7 cm radius, placed inside a 19 cm long cylindrical high density polyethylene moderator with 12.5 cm radius. The prompt gamma rays were detected by a 25.4 cm x 25.4 cm (thickness x diameter) NaI detector [20]. Figure 7 shows a prompt γ-rays spectrum (with gamma-ray energies in excess of 3 MeV) of a Portland cement concrete specimen containing 3 wt. % chloride, superimposed on a spectrum of pure Portland cement (lower curve). Due to contamination of chloride in Portland cement, additional full energy prompt γ-ray peaks from chloride are observed at 6.11 MeV. The single escape peak corresponding to 7.79 MeV full energy peak is also observed. Full energy and single escape peaks are labeled with letters F and S, respectively. The 6.11 MeV peaks had interference with calcium peak while single escape peak from 7.79 MeV peak had interference with iron doublet.

Another prompt gamma ray peak from chloride was observed at 1.17 (1.165) MeV. This peak is located in an isolated region with a linear-background and ideally suited for chloride concentration analysis. Figure 8 shows the enlarged view of the superimposed spectra of 1.17 MeV prompt γ-rays spectra for the Portland cement concrete specimen containing 1 wt % chloride (bottom most spectrum), 2 wt % chloride concentration (next to bottom most spectrum), 3 wt. % chloride concentration (next to top most spectrum) and 4 wt. % chloride concentration (top most spectrum) [20].

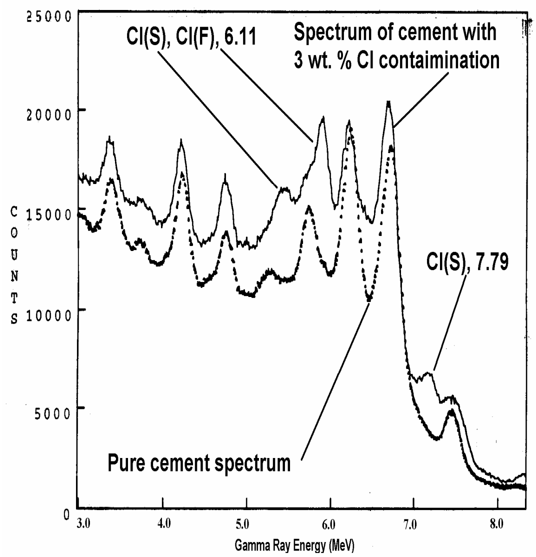

Figure 7: Prompt γ-ray spectrum of a Portland cement containing 3.0 wt. % chloride contamination superimposed on a spectrum for uncontaminated concrete specimen.

The integrated counts under the 1.17 MeV prompt gamma ray after background subtraction are plotted in Figure 9 as a function of chloride concentration in the Portland cement over 0.25-4 wt. % chloride concentration [20].

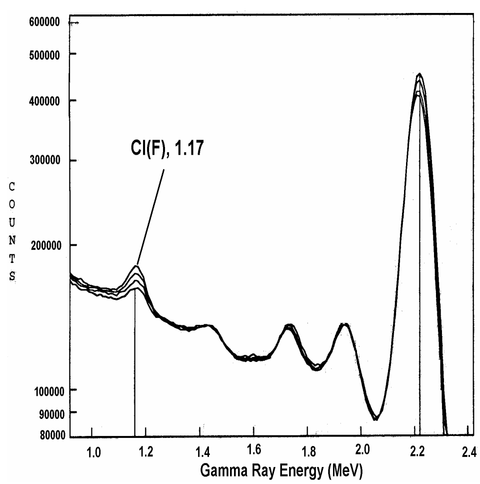

Figure 8: Spectra of 1.165 MeV γ-ray of chloride from the Portland cement concrete specimen containing 1 wt. % (bottom most), 2 wt % (next to bottom most), 3 wt.% (next to top most) and 4 wt. %(top most) chloride.

For comparison with experimental results, the yield of 1.17 MeV prompt gamma ray from chloride was calculated as a function of chloride concentration in the Portland cement. The calculated-normalized yield of the 1.17 MeV prompt gamma ray from chloride as a function of chloride concentration in Portland cement has been superimposed on the experimental data and is shown with a solid line in Figure 9. A good agreement could be noted between the experimental data and the calculated yield [20].

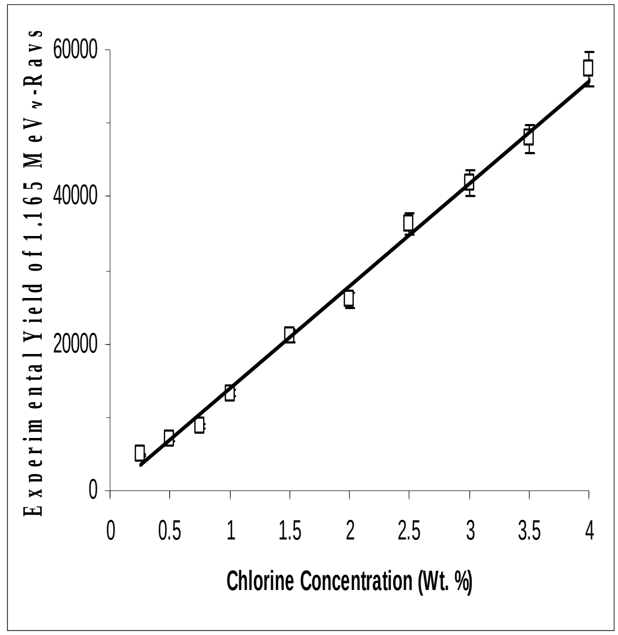

Figure 9 Experimentally measured yield of 1.165 MeV prompt gamma ray as a function of chloride concentration in Portland cement concrete specimen superimposed on the calculated yield.

5. Measurement of Lime to Silica Ratio in Concrete specimens

The lime/silica ratio was measured in six concrete specimens utilizing the KFUPM PGNAA setup [21]. The knowledge of this ratio is very important for durability of concrete structures. The lime/silica ratio in pre-mixing phase of concrete has been calculated from each sample ingredients and has been compared with the experimentally measured prompt gamma ray yield ratio of the respective elements in the specimen. From the mix composition of the six specimens, the elemental composition and the lime/silica ratio was calculated [21].

Figure 10 shows prompt gamma ray pulse height spectrum of specimen No. 3 superimposed upon the gamma ray pulse height spectrum of specimen No. 4 [21]. Specimen No. 3 has lower concentration of calcium but higher concentration of silicon than specimen No. 4. This is clearly demonstrated by the pulse height spectrum of specimen No. 3 (shown by solid line) and specimen No. 4 (shown by dotted line) shown in Figure 10. The experimental yield of calcium (1.94 MeV) and silicon (3.54 MeV) prompt gamma peaks in the pulse height spectra of all the six specimens was calculated. Then the experimental value of lime/silica ratio was calculated from the ratio of yield of 6.42

MeV gamma ray from calcium and 4.93 MeV gamma rays from silicon for each specimen and it is plotted in Figure 11 against calculated value of lime/silica ratio for each specimen [21]. A good agreement is noted between the experimental and theoretical value. It is worth mentioning here that the lime/silica ratio, which is plotted here is, the initial value in the pre-mixing phase. The ultimate lime to silica ratio in the concrete has different values and is needed to be determined through other techniques adopted by ASTM [9].

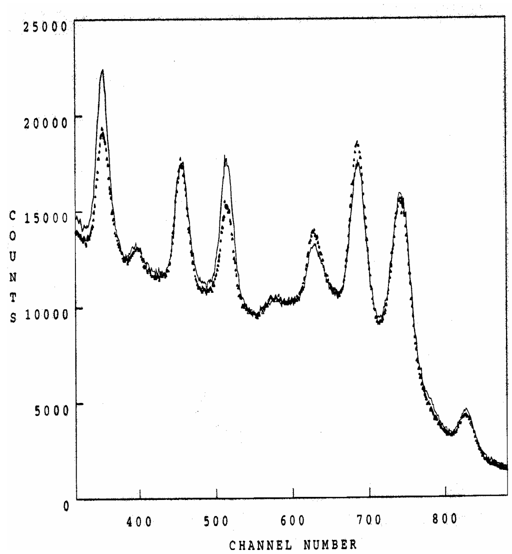

Figure 10: Experimentally measured prompt γ-rays spectra of the concrete specimens above 3 MeV for specimen No. 3 (shown with solid line) and sample No. 4 (shown with dashed line).

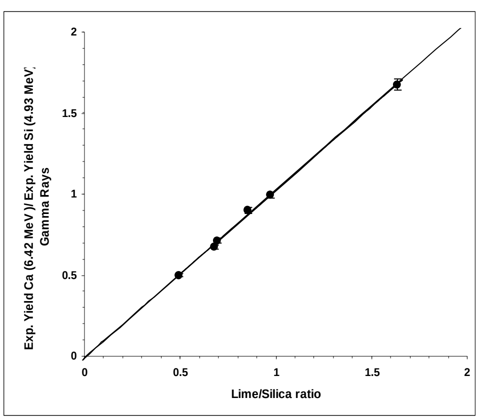

Figure 11: The ratio of experimental yield of 6.42 MeV prompt gamma rays from calcium and 4.93 MeV prompt gamma rays from silicon in each of six concrete specimens plotted as a function of corresponding lime/silica ratio of each specimen. The solid line shows normalized-calculated yield ratio of 6.42 MeV and 4.93 MeV gamma rays from the six concrete specimens obtained through Monte Carlo calculations.

6. Assessment of Chloride Concentration in Concrete Specimen

The chloride concentration in Portland concrete was measured from specimens containing 0.5, 1.0, 1.5, 2.0 and 3.0 wt. % of chloride [22, 23]. The chloride contaminated concrete specimens were prepared by mixing required sodium chloride with the other mix ingredients [22].

Figure 12 shows prompt γ-rays spectra of the four concrete specimens, above 3 MeV energy, containing 0.5, 1.5, 2.0 and 3 wt. % chloride superimposed upon each other [30]. The chloride has several capture gamma ray peaks and they interfere with gamma rays from concrete constituents. The chloride gamma rays with 6.110 and 6.619 MeV have been observed in the concrete pulse height spectra. The 6.619 MeV gamma ray peak from chloride (unlabelled) is located between the electronics sum peak and the full energy peak of the 6.42 MeV gamma ray from calcium in concrete. However, the 7.413 MeV gamma ray peak from chlorine is located in an isolated region. This peak can be used to extract chloride concentration information. For the 7.413 MeV chloride gamma ray peaks shown in the Figure 12, the top-most peak corresponds to 3 wt. % chloride concentration, while the bottom-most peak corresponds to 0.5 wt. %, next-to-top most peak corresponds to 2 wt. % chloride concentration, while next-to-bottom most peak corresponds to 1.5 wt. % chloride concentration [23].

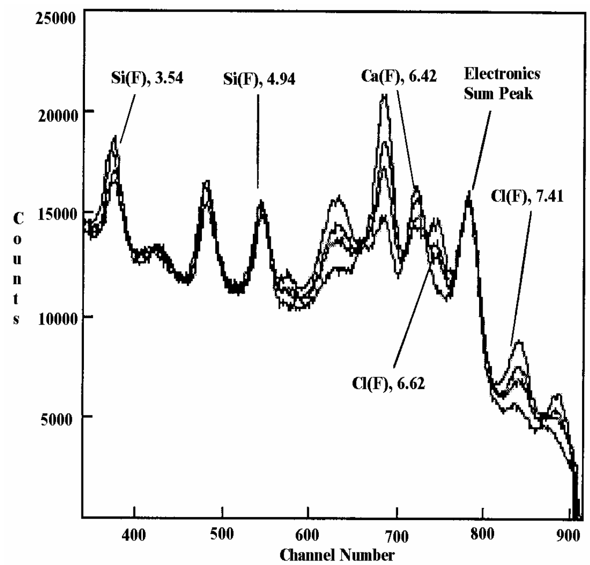

Figure12: Prompt γ-rays spectra of the concrete samples, above 3 MeV energy, containing 0.5, 1.5, 2.0 and 3 wt. % chloride.

As shown in Figure 13, the chloride peak at 1.165 MeV was also observed in this study as well. For the 1.164 MeV chloride gamma ray peaks shown in Figure 14, the top-most peak corresponds to 3 wt. % chloride concentration, while the bottom-most peak corresponds to 0.5 wt. %, next-to-top most peak corresponds to 2 wt. % chloride concentration while next-to-bottom most peak corresponds to 1.5 wt. % chlorine concentration [23].

Figure 14 shows the normalized-experimental yield of 7.413 MeV gamma-ray from chloride in the five concrete specimens as a function of the chloride concentration. The solid line in Figure 14 shows the normalized-calculated yield of the 7.413 MeV prompt gamma ray from chloride obtained through Monte Carlo simulations. Similarly,

Figure 15 shows the normalized-experimental yield of the 1.164 MeV prompt gamma ray from chloride in the five concrete specimens as a function of the chloride concentration. The solid line in Figure 15 shows normalized-calculated yield of the 1.164 MeV prompt gamma ray from chloride obtained through Monte Carlo simulations.

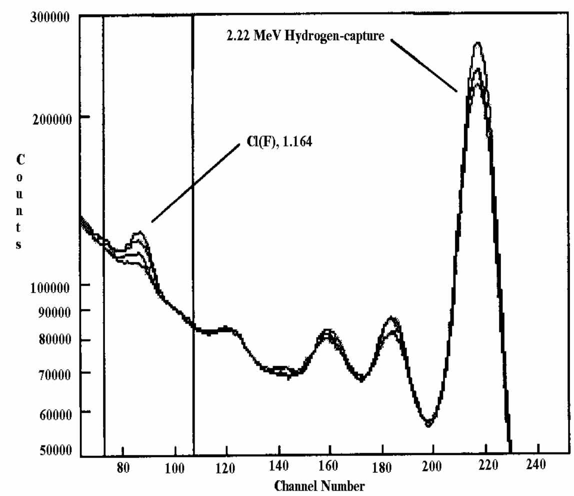

Figure 13: Prompt γ-rays spectra of the concrete specimens, below 3 MeV energy, containing 0.5, 1.5, 2.0 and 3 wt. % chlorine.

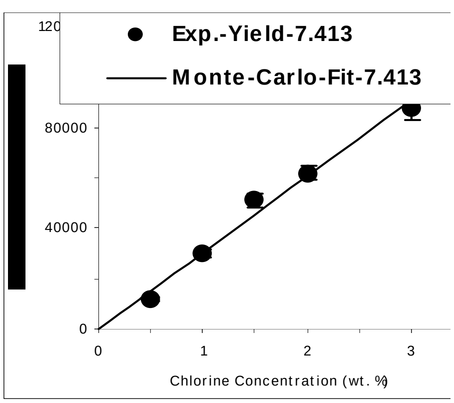

Figure 14: Experimental yield of 7.41 MeV prompt gamma rays from chloride in the five concrete specimens plotted as a function of chloride concentration.

The minimum detection limit of chloride in concrete was calculated for the KFUPM PGNAA setup using 1.165 and 7.413 MeV gamma rays from chloride in concrete. For both the 1.165 and 7.413 MeV gamma rays from chloride, the MDC limit was calculated to be 0.074 ±0.025 wt %, respectively [22]. The maximum permissible limit of chloride concentration in concrete set by ACI 318 is 0.03 wt. %. Within a statistical uncertainty of ±0.025 wt. %, the MDC lower bound of 0.048 wt. % for the KFUPM PGNAA setup is only 60 % higher than the maximum permissible limit of 0.03 wt. % of chloride set by ACI 318 [3]. If the KFUPM neutron source intensity is increased, MDC limit of chloride can be improved significantly to meet the standard [22].

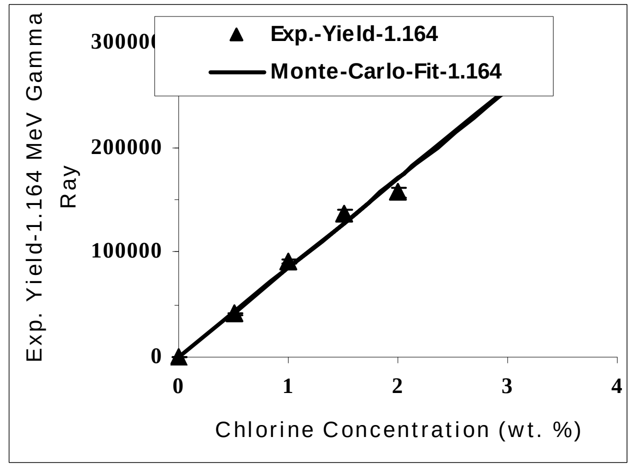

Figure 15: Experimental yield of 1.164 MeV prompt gamma rays from chloride in the five concrete specimens plotted as a function of chloride concentration.

7. Assessment of Sulfur in Concrete

The sulfur concentration was measured from concrete specimens containing 2.0, 4.0 and 6.0 wt. % weight proportion sulfur [22]. Figure 16 shows 5.421 MeV prompt gamma ray due to the capture of thermal neutrons in sulfur in the concrete specimens [22]. The 5.421 MeV peak location coincides with the double escape peak of calcium but the intensity of the double escape peak from calcium is insignificant (typically less than 0.5% of the full energy peak). The height of sulfur peak increases with sulfur concentration. The highest 5.421 MeV peak in Figure 16 corresponds to a 6 wt. % concentration, while the smallest peak corresponds to 2 wt. % and the middle one corresponds to 4 wt. %. The net counts under each peak of 5.421 MeV gamma ray in the four concrete specimens are plotted in Figure 17 as a function of the sulfur concentration. The solid lines in Figure 18 represent the calculated yield of the 5.421 MeV prompt gamma ray from the sulfur obtained through the Monte Carlo simulations [22].

The minimum detection limit of sulfur concentration in concrete MDC was calculated for the KFUPM PGNAA setup using the 5.421 MeV prompt gamma ray from the sulfur [22]. The MDC of sulfur in concrete was calculated to be 0.600±0.187 wt %. which is close to the minimum limit of 0.60 wt. % of sulfur in concrete set by BS 1880 [22].

Acknowledgement

The research presented in this paper was funded by King Fahd University of Petroleum and Minerals, Dhahran, Saudi Arabia, under Projects No. SABIC/2002-03 and IN060305.

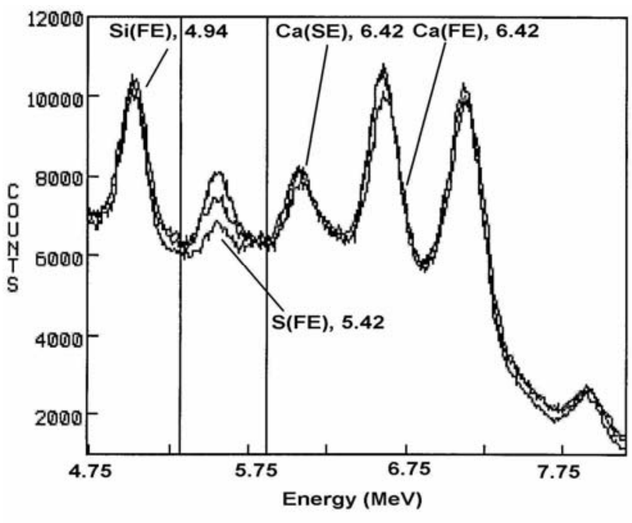

Figure 16: Prompt γ-rays spectra of the concrete specimens above 3 MeV energy, containing 2.0, 4.0 and 6.0 wt. % sulfur. The top most spectrum is for 6 wt. % sulfur concentration, middle one for 4 wt. % and bottom most spectrum for 2.0 wt % sulfur concentration.

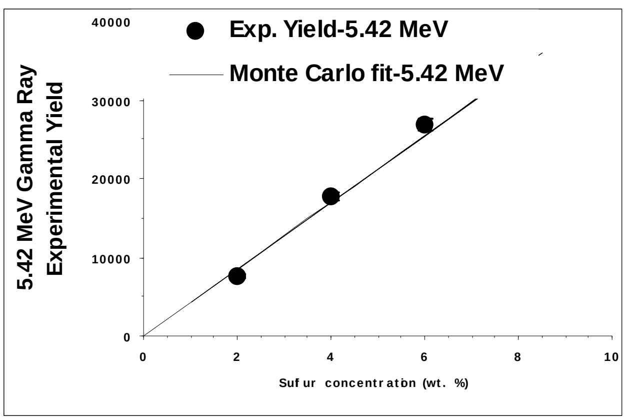

Figure 17: Experimental yield of 5.42 MeV prompt gamma rays from sulfur in four concrete specimens plotted as a function of sulfur concentration.

8. REFERENCES

[1] Maslehuddin M., Page C. L. and Rasheeduzzafar. *Journal of Materials in Civil Engineering*, 8 (1996), p. 63.

[2] Al-Amoudi, O.S.B., and Maslehuddin, M in *Concrete Repair, Rehabilitation and Protection*, R. K. Dhir and M.R. Jones (Editors), E & FN Spon, London, 1996, pp. 141-154.

[3] ACI Committee 222, Corrosion of Metals in Concrete, (ACI 222R-89), American Concrete Institute, Detroit, USA, 1989. Also: ACI Manuals of Concrete Practice, Part I.; ACI 318 Building Code Requirements for Structural Concrete (ACI 318-99) and Commentary (ACI 318R-99), American Concrete Institute, Farmington Hills, USA, 1999.

[4] Maslehuddin, M. and Al-Amoudi , O.S.B., "Corrosion of Reinforcing Steel in Concrete: Its Monitoring and Prevention," Proceedings, Symposium on Corrosion and Its Control, King Saud University, Riyadh, Saudi Arabia, May 1992, pp. 110-125.

[5] Al-Amoudi, O.S.B.; Maslehuddin, M., and Bader, M.A., Characteristics of Silica Fumes and its Impact on Concrete in the Arabian Gulf , *Concrete*, Vol. 35, No. 2, February 2001, pp. 45-50.

[6] Al-Amoudi, O.S.B., Durability of Plain and Blended Cements in Marine Environments, *Advances in Cement Research*, Vol. 14, No. 3, July 2002, pp. 89-100.

[7] PCI Committee, Guide to Using Silica Fumes in Precast/Prestressed Concrete Products, *PCI Journal*, Vol. 39, No. 5, September-October 1994, pp. 36-45.

[8] Al-Amoudi, O. S. B. " Durability of Plain and Blended Cements in Marine Environments", Advances in Cement Research, Vol. 14, No. 3, 2002, pp.89-100.

[9] Test Methods for Chemical Analysis of Cement, ASTMC-114. Published by American Society for Testing of Materials, Philadelphia, USA.

[10] Vogel I. A., A Textbook of Quantitative Inorganic Analysis, 5th Edition, Revised by J. Basset, Longman, London, 1985.

[11] B. D. Sowerby and J. S. Watt; "Nuclear Techniques for On-line Analysis in the Minerals and Energy Industries, ". Proceedings, 9th Pacific Basin Nuclear Conference, Sydney, Australia; 1994. pp. 379

[12] Saleh H. H. and Livingston, R. A. Experimental Evaluation of a Portable Neutron-Based Gamma- Spectroscopy System for Chloride Measurements in Reinforced Concrete. J. Radioanal. Nucl. Chem., Vol.244 (2000) 367.

[13] Daniel L. Collico Savio, Mario A. J. Mariscotti and Sergio Ribeiro Guevara. Elemental Analysis of a concrete sample by capture gamma rays with a radioisotope neutron source. Nuclear Instruments & Methods in Physics Research B 95 (1995), pp. 379-388.

[14] Khelifi R., Idiri Z., Omari L.and Seghir M.. Prompt Gamma Neutron Activation Analysis of Bulk Concrete Samples with an Am-Be Neutron Sources. Applied Radiation and Isotopes, Vol. 51 (1999) 9.

[15] Tickner J. Determination of the Spatial Response of Neutron Based Analyzers using a Monte Carlo Based Method. Applied Radiation and Isotopes Vol. 53(2000), 507.

[16] Lim C. S., Tickner J. R., Sowerby B. D., Abernethy D. A., McEwan A. J., Rainey S., Stevans R., Manias C., Retallack D. An On-belt Elemental Analyzer for the Cement Industry. Applied Radiation and Isotopes. Vol. 54(2001)11.

[17] Naqvi, A. A., M. M. Nagadi, Khateeb-ur-Rehman, M. Maslehuddin and S. Kidwai.. Monte Carlo simulations for the design of the KFUPM PGNAA facility. Rad. Phys. Chem. 66(2) (2003) 89.

[18] Naqvi A. A., Fazal-ur-Rehman, Al-Jarallah M.I., F. Abu-Jarad and M. Maslehuddin. Performance Tests of External Moderators of a PGNAA Setup. Applied Radiation Isotopes. Vol. 58 (2003) pp. 27-38.

[19] Naqvi A. A., M. M. Nagadi and O. S. B Al-Amoudi. Elemental analysis of concrete samples using an accelerator-

based PGNAA setup. Nuclear Instruments & Methods in Physics Research B Vol. 225/3 (2004) pp. 331-338.

[20] Naqvi, A. A., M. M. Nagadi, S. Kidwai, Khateeb-ur-Rehman and M. Maslehuddin. "Search of a Prompt Gamma Ray for Chlorine Analysis in a Portland Cement Sample. Nuclear Instruments & Methods in Physics Research A 533/3 (2004) pp. 591-597

[21] Naqvi A. A., M. M. Nagadi and O. S. B. Al-Amoudi. Measurement of lime/silica ratio in concrete samples using PGNAA technique. Nuclear Instruments & Methods in Physics Research A Volume 554, Issues 1-3, 1 December (2005), Pages 540-545

[22] Naqvi A. A., M. M. Nagadi and O. S. B. Al-Amoudi; Gamma rays Interferences in Corrosion Analysis of Concrete Samples. Nuclear Instruments & Methods in Physics Research A, Vol. 569/3 (2006) pp 803-809.

[23] Naqvi A. A., M. M. Nagadi and O. S. B. Al-Amoudi. Prompt Gamma Analysis of Chlorine in Concrete for Corrosion Study. Applied Radiation and Isotopes, Vol. 64/2 (2006) pp 283-289.

[24] Naqvi A. A, M. M. Nagadi , M. A. Garwan, O.S. B. Al-Amoudi[2] and M. Maslehuddin; Prompt Gamma Ray Analysis of Fly Ash Cement Based Concrete Samples. Paper presented in SECOND INTERNATIONAL NUCLEAR CHEMISTRY CONGRESS 2nd-INCC held at CANCUN, Mexico on April 13-18, 2008 pp. 65-Ry-3